

# Long-Range Neural Atom Learning for Molecular Graphs

Xuan Li<sup>1\*</sup> Zhanke Zhou<sup>1\*</sup> Jiangchao Yao<sup>2,3</sup> Yu Rong<sup>4</sup> Lu Zhang<sup>1</sup> Bo Han<sup>1</sup>

<sup>1</sup>Hong Kong Baptist University <sup>2</sup>CMIC, Shanghai Jiao Tong University

<sup>3</sup>Shanghai AI Laboratory <sup>4</sup>Tencent AI Lab

{csxuanli, cszkzhou, ericluzhang, bhanml}@comp.hkbu.edu.hk  
sunarker@sjtu.edu.cn yu.rong@hotmail.com

## Abstract

Graph Neural Networks (GNNs) have been widely adopted for drug discovery with molecular graphs. Nevertheless, current GNNs are mainly good at leveraging short-range interactions (SRI) but struggle to capture long-range interactions (LRI), both of which are crucial for determining molecular properties. To tackle this issue, we propose a method that implicitly projects all original atoms into a few *Neural Atoms*, which abstracts the collective information of atomic groups within a molecule. Specifically, we explicitly exchange the information among neural atoms and project them back to the atoms' representations as an enhancement. With this mechanism, neural atoms establish the communication channels among distant nodes, effectively reducing the interaction scope of arbitrary node pairs into a single hop. To provide an inspection of our method from a physical perspective, we reveal its connection with the traditional LRI calculation method, Ewald Summation. We conduct extensive experiments on three long-range graph benchmarks, covering both graph-level and link-level tasks on molecular graphs. We empirically justify that our method can be equipped with an arbitrary GNN and help to capture LRI.

## 1 Introduction

Graph Neural Networks (GNNs) show promising ability of modeling complex and irregular interactions [30; 22; 34]. In particular, GNNs attract growing interest in accelerating drug discovery due to the accurate prediction of the molecular properties [20; 10; 27; 16; 35].

The basic elements of a molecule are different types of atoms, while the interactions among atoms can be generally categorized into short-range interactions (SRI) and long-range interactions (LRI). Wherein, SRI, such as covalent bonds or ionic bonds, acts over relatively *small distances* that are typically within the range of a few atomic diameters. By contrast, LRI, such as hydrogen bonds and coulombic interactions, operates over *much larger distances* compared to the typical atomic diameter. Although LRI is typically with weaker strength than SRI, it plays a significant role in determining the physical and chemical properties of molecules [28; 15].

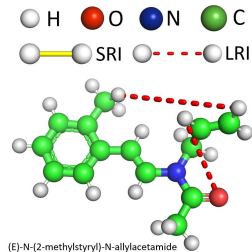


Figure 1: An exemplar molecular with the long-range interactions (dash lines) and short-range interactions (solid lines).

\*Equal contributions.

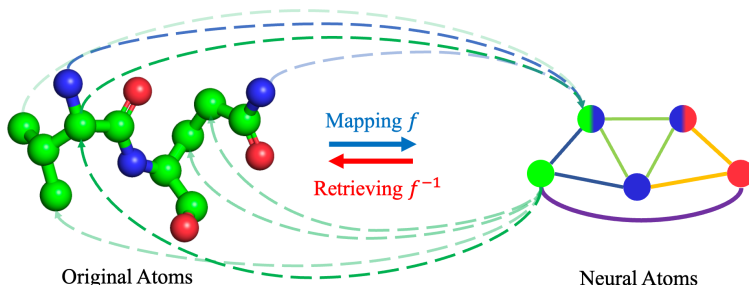


Figure 2: Illustration of *Neural Atoms*. The mapping function  $f$  is to project the original atoms to *Neural Atoms*, and the retrieving function  $f^{-1}$  aims to inject the information of *Neural Atoms* to original atoms, allowing the GNN model to capture LRI via the interaction between *Neural Atoms*.

In Fig. 1, we give an illustration of SRI and LRI in a molecular graph, which is formed by the covalent bonds with explicit hydrogens. The SRIs here, *e.g.*, the covalent bond between carbon (●) and hydrogen (○), are denoted as solid lines (●—○), which involves the electron exchange of atoms to establish the stabilization of the molecular structure. As such, the SRIs are considered to be the explicit edges of the molecular graph. On the other hand, the LRIs (denoted as dashed lines) are in the form of the implicit force depending on the distance between atoms in the 3D range and the molecular structure, and could involve atoms with multiple hops distance. For example, the hydrogen bond (○, ●) can involve the 5-length path (○, ●, ●, ●, ●, ●) with four middle atoms, whereas the hydrogen bond (○, ○) can involve the long path (○, ●, ●, ●, ●, ●, ●, ●, ●, ●, ○) of length 10, with nine middle atoms.

GNNs can effectively capture the SRI as they aggregate neighboring information in each layer, however, they are intrinsically ineffective in capturing the LRI that is located among distant nodes. Naively stacking more layers to perceive LRI will encounter exponentially increasing neighbor nodes. This induces GNN to compress excessive spurious information of some irrelevant long-range neighbor nodes, which results in the well-known over-squashing problem [1]. A common enhancement of GNNs is Graph Transformer (GT) [13; 14], which uses the self-attention mechanism to process information from neighbors that allows the capture of complex and long-range relationships between nodes. However, with self-attention, a node may attend to a large number of nodes with no direct edge connection, where the excessive information hinders the capturing of meaningful and sparse LRI. In practice, GTs only achieve marginal improvements compared with GNNs [26], while the self-attention on the entire molecule makes GTs much more computationally expensive than GNNs.

In this work, we aim to design an effective and efficient mechanism to enhance GNNs for capturing long-range interactions. We notice that in areas of computational chemistry and molecular modeling, the pseudo atoms can be employed to group atoms into a more manageable and computationally efficient representation. Note these pseudo atoms are not real atoms with physical properties but are introduced for simplification and convenience in calculations. One can approximate the effects of LRIs by introducing pseudo atoms strategically, making simulations of complex molecular systems more tractable while still retaining the essential characteristics of these interactions. However, pseudo atoms cannot be directly applied here, as they are typically manually designed with expert knowledge.

To close this gap, we propose *Neural Atoms: Learning to implicitly project all the original atoms into a few neural atoms* that abstract the collective information of atomic groups in a molecule. Based on this, we explicitly exchange the information among neural atoms and project them back to the atoms’ representations as an enhancement. Under this mechanism, the neural atoms establish the communication channels among distant nodes, which can reduce the interaction scope of arbitrary node pairs into a single hop. Note that the proposed method is architecture-agnostic and computation-efficient, which can be equipped with an arbitrary GNN and help to capture LRI. Empirically, we evaluate our method on three long-range graph benchmarks [26] with both link-level and graph-level tasks. We achieve up to 27.32% improvement in the Peptides-struct dataset with different kinds of commonly-used GNNs. Our main contributions are summarized as follows.

- We formalize the concept of neural atoms, and instantiate it with dual self-attention mechanisms to learn the atoms-neural atoms projection and model the interactions among neural atoms (Sec. 3).
- We conduct extensive experiments on long-range molecular datasets for property prediction and structure reconstruction, and empirically justify that our method can boost various GNNs (Sec. 4).

- We provide an in-depth understanding of our method from a physical perspective and reveal its intrinsic connection with a commonly-used LRI calculation method, Ewald Summation (Sec. 5).

## 2 Preliminaries

**Notation.** An undirected graph is denoted as  $\mathcal{G} = (\mathcal{V}, \mathcal{E})$ , where  $\mathcal{V}$  is the node set and  $\mathcal{E}$  is the edge set. For each node  $v \in \mathcal{V}$ , its  $D$ -dimension node feature is denoted as  $x_v \in \mathbb{R}^D$ . Besides,  $\mathbf{h}_v^{(\ell)}$  denote the node representation of node  $v$  in  $\ell$ -th layer for a  $L$ -layer GNNs, where  $0 \leq \ell \leq L$  and  $\mathbf{h}_v^{(0)} = x_v$ .

**Graph Neural Networks.** Given a graph  $\mathcal{G}$ , the neighbor information aggregate function  $f^{(\ell)}$  and the node representation update function  $\phi^{(\ell)}$ , we can formulate the  $\ell$ -th layer operation of GNNs as

$$\mathbf{h}_v^{(\ell)} = \phi^{(\ell)}\left(\mathbf{h}_v^{(\ell-1)}, f^{(\ell)}(\mathbf{h}_v^{(\ell-1)})\right),$$

where  $\mathcal{N}(v) = \{u \in \mathcal{V} | (u, v) \in \mathcal{E}\}$  are the neighbor nodes of node  $v$ . Different GNNs vary from the design of the function  $f^{(\ell)}$  and  $\phi^{(\ell)}$ . For example, GCN [11] define its  $f^{(\ell)}$  as

$$f^{(\ell)}(\mathbf{h}_v^{(\ell-1)}) = \sum_{u \in \mathcal{N}(v) \cup \{v\}} 1/\sqrt{\hat{d}_u \hat{d}_v} \mathbf{W}^{(\ell)} \mathbf{h}_u^{(\ell-1)},$$

and use ReLU function as  $\phi^{(\ell)}$ , where  $\mathbf{W}$  is the learnable parameter for filtering the graph signal. Likewise, GIN [31] obtain neighbor information by  $f^{(\ell)}(\mathbf{h}_v^{(\ell-1)}) = \sum_{u \in \mathcal{N}(v) \cup \{v\}} \mathbf{h}_u^{(\ell-1)}$ , and update node representation via a feed-forward network. In addition, the node representations in the last GNN layer would then be transformed by a feed-forward network for specific downstream tasks. For example, for graph-level classification tasks, the whole representations  $\mathbf{H} \in \mathbb{R}^{N \times d}$  would be transformed to the logits  $\hat{\mathbf{Y}} \in \mathbb{R}^C$  with  $C$  classes that usually through the graph pooling operation.

**Multi-head Attention Mechanism.** Consider a molecular graph with  $N$  nodes, the input of the attention mechanism  $f_{\text{Att}}$  consists of three components, termed as query  $\mathbf{Q} \in \mathbb{R}^{k \times d_k}$ , key  $\mathbf{K} \in \mathbb{R}^{N \times d_k}$ , and value  $\mathbf{V} \in \mathbb{R}^{N \times d_v}$ , where  $d_k$  and  $d_v$  are dimensions. As such, the  $f_{\text{Att}} = \sigma(\mathbf{Q}\mathbf{K}^T)\mathbf{V}$  is calculated via the dot product of the query and the key, with  $\sigma$  denoting the activation function. To extend the attention to the multi-head case, we further utilize the linear projection for  $\mathbf{Q}$ ,  $\mathbf{K}$ , and  $\mathbf{V}$  to yield  $M$  representation subspace. The multi-head attention mechanism allows us to learn different attentions between query and key, thus enhancing the model expressivity. Namely, with  $M$  attention heads,

$$\text{MultiHead}(\mathbf{Q}, \mathbf{K}, \mathbf{V}) = \mathbf{W}^O \parallel_{m=1}^M \mathbf{O}_m, \quad \text{s.t. } \mathbf{O}_m = f_{\text{Att}}(\mathbf{Q}\mathbf{W}_m^Q, \mathbf{K}\mathbf{W}_m^K, \mathbf{V}\mathbf{W}_m^V),$$

where  $\mathbf{W}^O \in \mathbb{R}^{M d_h \times d_{out}}$  is the linear projection matrix for learning the subspace representation of the contracted head outputs to output dimension  $d_{out}$ . Besides,  $\mathbf{W}_m^Q \in \mathbb{R}^{d_k \times d_k}$ ,  $\mathbf{W}_m^K \in \mathbb{R}^{d_k \times d_k}$ , and  $\mathbf{W}_m^V \in \mathbb{R}^{d_v \times d_v}$  are the projection matrixes in the  $m$ -th head for query, key, and value, respectively.

**Graph Hierarchical Learning.** The GNNs can only propagate information through edges formed by the SRI. To capture LRI, the model would inevitably aggregate information on the numerous intermediate atoms from the source node to the target node. The overwhelming information could suppress the information from distant target nodes, thus degenerating the ability of the model to capture LRI. An intuitive idea is to group the intermediate atoms and abstract their information into a single node. This could reduce the information propagating length of LRI by decreasing the potential intermediate atoms, which helps to enhance the information strength of the distant atoms. The grouping operation is achieved by graph pooling for abstracting the node representation while preserving the local structure information [33; 18; 6; 3]. Such an operator allows the model to obtain multi-scale graph-level representation, which implicitly enhances the model to capture LRI. However, the graph pooling is designed for obtaining global graph representation, without considering cooperating with the LRI and SRI information. It makes the GNN model unable to propagate and utilize the LRI information.

**Graph Laplacian Position Encoding.** The position encoding can benefit graph learning by instilling distinguishable information to the node features, such as local structure and Laplacian eigenvectors [14]. Standard GNNs are known to be bounded by the 1-Weisfeiler-Leman test (1-WL), meaning they fail to distinguish non-isomorphic graphs with 1-hop message passing. Instilling graph position encoding allows GNNs to be more expressive than the 1-WL test, as each node is equipped with the distinguishable information [13; 14].

**Ewald Summation.** The Ewald Summation [23] is a calculation algorithm for molecular dynamics simulation, which calculates the energy of the interaction by processing the atoms' position and their

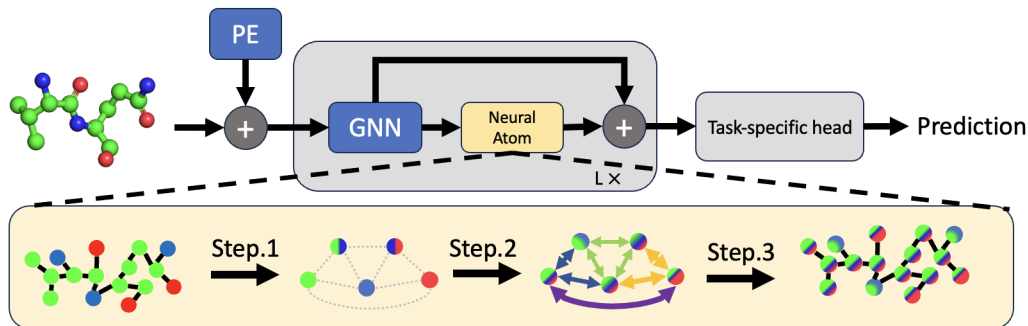


Figure 3: The proposed Neural Atom framework aims to obtain graph representation for different downstream tasks. The Neural Atom can enhance arbitrary by injecting LRI information via the interaction of neural atoms. We demonstrate the information exchange by the mixture of colors.

charges via mathematical models. The Ewald Summation decomposes the actual interaction into the short-range and the long-range part, where the former decays vastly in the real space, and the latter would only exhibit fast decay in the frequency space. The short-range part can be calculated by employing a summation with the distance cut-off. Whereas the long-range part, transformed by Fourier transformation, can be calculated via a low-frequency cut-off summation. A similar approach [12] enhances standard GNN with Ewald Summation, which allows the model to calculate LRI efficiently and produce more accurate 3D molecular simulation.

### 3 Method

In this section, we first introduce the concept of neural atoms and how it can benefit GNNs to capture LRI (Sec. 3.1). Next, we elaborate on the attention-based approach to realize neural atoms (Sec. 3.2). Finally, we connect it with the Ewald Summation from the graph representation learning (Sec. 3.3).

#### 3.1 Formalizing the Neural Atoms on Molecular Graphs

As aforementioned, we proposed the neural atoms inspired by the pseudo-atoms of molecular dynamics simulations, which abstract prefixed atom groups into individual representations. By mapping the atoms into neural atoms and allowing a fully connected structure with neural atoms, one can reduce the LRI into direct neighbor interaction. The formalization of neural atoms is as follows.

**Definition 3.1.** *Neural atoms encompass a collection of virtual and adaptable atoms that symbolize a cluster of atoms within a designated molecular graph. The process entails the acquisition of knowledge that enables the transformation of conventional atoms into neural atoms. This transformation can be technically executed through methodologies such as graph clustering or graph coarsening.*

**Advantages.** Different neural atoms are designed to gather data from distinct local regions, with the intent of preserving local information to the greatest extent possible. This approach serves to alleviate the challenges associated with learning intricate graph structures. Consequently, interactions among atoms that are widely separated are transformed into interactions among neural atoms, effectively narrowing the interaction range from any arbitrary pair of atoms to a single step, as illustrated in Fig. 2. Employing a layer-wise collaboration with GNNs, information from distant atoms can be effectively exchanged through the interactions among neural atoms. In what follows we elaborate on the implementation of neural atoms via the attention mechanism and the collaboration with GNNs.

#### 3.2 Injecting long-range information into message passing by neural atoms

The overall inference pipeline is illustrated in Fig. 3. Specifically, in  $\ell$ -th layer, we obtain the atom representations  $\mathbf{H}_{\text{GNN}}^{(\ell)}$  with neighborhood information via the  $\ell$ -th GNN layer. Then, we apply neural atoms to enhance the representations as  $(\mathbf{H}_{\text{GNN}}^{(\ell)}, \mathbf{H}_{\text{NA}}^{(\ell)}) \rightarrow \mathbf{H}^{(\ell)}$ , which includes three steps as follows.

**Step1. Project atom representations  $\mathbf{H}_{\text{GNN}}^{(\ell)}$  to neural atom representations  $\mathbf{H}_{\text{NA}}^{(\ell)}$ .** To achieve this projection, we commence by initializing a learnable neural atom weights  $\mathbf{Q}_{\text{NA}}^{(\ell)} \in \mathbb{R}^{K \times d_k}$ , where

$K$  ( $\ll N$ ) specifies the number of neural atoms as a hyperparameter and  $d_k$  is the embedding dimension. By employing the multi-head attention (MultiHead), we can learn the grouping function for obtaining neural atoms representing the intermediate atoms. Wherein, the atom representations  $\mathbf{H}_{\text{GNN}}^{(\ell)} \in \mathbb{R}^{N \times d}$  are mapped to the key  $\mathbf{K} \in \mathbb{R}^{N \times d_h}$  and value  $\mathbf{V} \in \mathbb{R}^{N \times d_h}$  by linear projection weights  $\mathbf{W}_K \in \mathbb{R}^{d_h \times d_h}$  and  $\mathbf{W}_V \in \mathbb{R}^{d_h \times d_h}$ , respectively. The allocation matrix  $\hat{\mathbf{A}}_m$  for  $m$ -th head is obtained as  $\hat{\mathbf{A}}_m = \sigma(\mathbf{Q}_{\text{NA}}^{(\ell)} \mathbf{K}^\top) \in \mathbb{R}^{K \times N}$ , and  $\oplus$  denotes operation for combining representations, *e.g.*, sum or a feed forward network. The representations  $\mathbf{H}_{\text{NA}}^{(\ell)}$  of neural atoms are obtained by:

$$\mathbf{H}_{\text{NA}}^{(\ell)} = \text{LayerNorm} \left( \mathbf{Q}_{\text{NA}}^{(\ell)} \oplus \text{MultiHead}(\mathbf{Q}_{\text{NA}}^{(\ell)}, \mathbf{H}_{\text{GNN}}^{(\ell)}, \mathbf{H}_{\text{GNN}}^{(\ell)}) \right), \quad (1)$$

where the LayerNorm represents the operation of Layer Normalization [2].

**Step2. Exchange information among neural atoms  $\mathbf{H}_{\text{NA}}^{(\ell)} \rightarrow \tilde{\mathbf{H}}_{\text{NA}}^{(\ell)}$ .** Then, we explicitly exchange the information among neural atoms to capture the long-range interactions in this molecular graph. We further employ the self-attention mechanism for efficient information exchange, namely,

$$\tilde{\mathbf{H}}_{\text{NA}}^{(\ell)} = \text{LayerNorm} \left( \mathbf{H}_{\text{NA}}^{(\ell)} \oplus \text{MultiHead}(\mathbf{H}_{\text{NA}}^{(\ell)}, \mathbf{H}_{\text{NA}}^{(\ell)}, \mathbf{H}_{\text{NA}}^{(\ell)}) \right). \quad (2)$$

**Step3. Project neural atoms back and enhance the atoms' representation  $(\mathbf{H}_{\text{GNN}}^{(\ell)}, \mathbf{H}_{\text{NA}}^{(\ell)}) \rightarrow \mathbf{H}^{(\ell)}$ .** So far, the obtained  $\tilde{\mathbf{H}}_{\text{NA}}^{(\ell)}$  contains information from different atom groups. To cooperate the  $\tilde{\mathbf{H}}_{\text{NA}}^{(\ell)}$  with the original molecular atom, we aggregate the allocation matrix  $\hat{\mathbf{A}}_m$  of different heads and project the neural atoms into the atom space with size  $N$ . Here, we perform the matrix reduction operations (*e.g.*, mean or summation) to aggregate the multi-head  $\hat{\mathbf{A}}_m$  and get  $\tilde{\mathbf{A}}_{\text{NA}}^{(\ell)}$ , which allows the model to learn different allocation weights. The final atom representations  $\mathbf{H}^{(\ell)}$  are obtained by enhancing the atom representations  $\mathbf{H}_{\text{GNN}}^{(\ell)}$  with the neural atoms' representations  $\tilde{\mathbf{A}}_{\text{NA}}^{(\ell)} \tilde{\mathbf{H}}_{\text{NA}}^{(\ell)}$ , *i.e.*,

$$\mathbf{H}^{(\ell)} = \mathbf{H}_{\text{GNN}}^{(\ell)} \oplus \tilde{\mathbf{A}}_{\text{NA}}^{(\ell)} \tilde{\mathbf{H}}_{\text{NA}}^{(\ell)}, \quad \text{s.t. } \tilde{\mathbf{A}}_{\text{NA}}^{(\ell)} = \text{Aggregate}(\{\hat{\mathbf{A}}_m\}_{m=1}^M)^\top \in \mathbb{R}^{N \times K}. \quad (3)$$

**The overall procedure.** We summarize the forward pipeline in Algorithm 1. In brief, given the atom representations of a molecular graph  $\mathbf{H}_{\text{GNN}}^{(\ell-1)}$  in  $(\ell-1)$ -th layer, we first get the updated atoms' representations  $\mathbf{H}_{\text{GNN}}^{(\ell)}$  by the GNN in  $\ell$ -th layer to capture the SRI. Then, the atoms  $\mathbf{H}_{\text{GNN}}^{(\ell)}$  are projected to neural atoms  $\tilde{\mathbf{A}}_{\text{NA}}^{(\ell)} \tilde{\mathbf{H}}_{\text{NA}}^{(\ell)}$  to capture the LRI with the three above steps. Finally, the enhanced representations  $\mathbf{H}^{(\ell)}$  are obtained by mixing both atoms' and neural atoms' representations.

---

**Algorithm 1** Message propagation with neural atoms.

---

**Require:** Molecular graph  $\mathcal{G}$ , atoms feature  $X$ , and GNN model  $f$ .

- 1: Initialize  $\mathbf{H}^{(0)} \leftarrow X$
  - 2: **for**  $\ell = 1 \dots L$  **do**
  - 3:    $\mathbf{H}_{\text{GNN}}^{(\ell)} \leftarrow f^{(\ell)}(\mathbf{H}^{(\ell-1)}, \mathcal{G})$
  - 4:    $\mathbf{H}_{\text{NA}}^{(\ell)} \leftarrow \text{LayerNorm} \left( \mathbf{Q}_{\text{NA}}^{(\ell)} \oplus \text{MultiHead}(\mathbf{Q}_{\text{NA}}^{(\ell)}, \mathbf{H}_{\text{GNN}}^{(\ell)}, \mathbf{H}_{\text{GNN}}^{(\ell)}) \right)$
  - 5:    $\tilde{\mathbf{H}}_{\text{NA}}^{(\ell)} \leftarrow \text{LayerNorm} \left( \mathbf{H}_{\text{NA}}^{(\ell)} \oplus \text{MultiHead}(\mathbf{H}_{\text{NA}}^{(\ell)}, \mathbf{H}_{\text{NA}}^{(\ell)}, \mathbf{H}_{\text{NA}}^{(\ell)}) \right)$
  - 6:    $\tilde{\mathbf{A}}_{\text{NA}}^{(\ell)} \leftarrow \text{Aggregate}(\{\hat{\mathbf{A}}_m\}_{m=1}^M)^\top$
  - 7:    $\mathbf{H}^{(\ell)} \leftarrow \mathbf{H}_{\text{GNN}}^{(\ell)} \oplus \tilde{\mathbf{A}}_{\text{NA}}^{(\ell)} \tilde{\mathbf{H}}_{\text{NA}}^{(\ell)}$ ,
  - 8: **end for**
  - 9: **return**  $\mathbf{H}^{(L)}$ .
- 

### 3.3 Connection to the Ewald Summation

Here, we utilize the aforementioned Ewald sum matrix [7] to show and understand the interaction among particles. Each element in the matrix represents the corresponding Ewald summation, which offers a more rapidly converging series that ensure accurate results even for distant interactions. Specifically, the Ewald summation decomposes the interatomic interaction into short-range and long-range parts. Wherein, the short-range interaction (denoted as  $x_{ij}^{(r)}$ ) can be straightforwardly

Table 1: Dataset statistical information. All the datasets consist of molecular graphs that exhibit LRI.

Dataset	Total Graphs	Total Nodes	Avg Nodes	Mean Deg.	Total Edges	Avg Edges	Avg Short.Path.	Avg Diameter
pcqm-contact	529,434	15,955,687	30.14	2.03	32,341,644	61.09	4.63±0.63	9.86±1.79
pepfunc	15,535	2,344,859	150.94	2.04	4,773,974	307.30	20.89±9.79	56.99±28.72
pepstruct	15,535	2,344,859	150.94	2.04	4,773,974	307.30	20.89±9.79	56.99±28.72

summed by imposing a distance cutoff; while the long-range component (termed as  $x_{ij}^{(\ell)}$ ) exhibits a rapid decay in its Fourier transform although diminishing slowly with distance, *i.e.*,

$$x_{ij} = \underbrace{Z_i Z_j \sum_{\mathbf{L}} \frac{\text{erfc}(a \|\mathbf{r}_i - \mathbf{r}_j + \mathbf{L}\|_2)}{\|\mathbf{r}_i - \mathbf{r}_j + \mathbf{L}\|_2}}_{\text{SRI: } x_{ij}^{(r)}} + \underbrace{\frac{Z_i Z_j}{\pi V} \sum_{\mathbf{G}} \frac{e^{-\|\mathbf{G}\|_2^2 / (2a)^2}}{\|\mathbf{G}\|_2^2} \cos(\mathbf{G} \cdot (\mathbf{r}_i - \mathbf{r}_j))}{\pi V}}_{\text{LRI: } x_{ij}^{(\ell)}} + x_{ij}^{(s)}$$

The above equation gives the interatomic interaction strength, *i.e.*, the non-diagonal elements in the Ewald sum matrix. The  $Z_i$  and  $\mathbf{r}_i$  are the atomic number and position of the  $i$ -th atom, and  $V$  is the unit cell volume. Besides,  $L$  denotes the lattice vectors within the distance cutoff,  $G$  is the non-zero reciprocal lattice vectors, and  $a$  is the hyperparameter that controls the summation converge speed.

The strength of SRI and LRI are determined by multiplying the atomic numbers, which indicate the number of positive charges. The difference lies in the manner of calculating the distance between atoms. The  $x_{ij}^{(r)}$ , corresponding to the strength of the interaction in the real space, is calculated by the error function  $\text{erfc}$  and the Euclidian distance  $\|\mathbf{r}_i - \mathbf{r}_j + \mathbf{L}\|_2$  between atoms. The  $x_{ij}^{(\ell)}$  describe the interaction strength in the reciprocal space, which is calculated by the distance given by the dot product of  $G$  and the interatomic distance  $(\mathbf{r}_i - \mathbf{r}_j)$ . Whereas the self-energy  $x_{ij}^{(s)}$  is a constant term for the interaction from the positive atomic cores, which is irrelevant to the interatomic distance.

**Remark 3.1.** Recall in Eqn. (3), the final atom representations  $\mathbf{H}^{(\ell)}$  are obtained by combining both the atoms' representations  $\mathbf{H}_{\text{GNN}}^{(\ell)}$  and the neural atoms' representations  $\tilde{\mathbf{A}}_{\text{NA}}^{(\ell)} \tilde{\mathbf{H}}_{\text{NA}}^{(\ell)}$ . In association with the Ewald summation, The  $\mathbf{H}_{\text{GNN}}^{(\ell)}$  contains the information of the SRI term  $x_{ij}^{(r)}$  and self-energy term  $x_{ij}^{(s)}$  of the Ewald summation, while the enhanced  $\tilde{\mathbf{A}}_{\text{NA}}^{(\ell)} \tilde{\mathbf{H}}_{\text{NA}}^{(\ell)}$  is to approximate the LRI term  $x_{ij}^{(\ell)}$ .

## 4 Experiments

In this section, we empirically evaluate the proposed method on real-world molecular graph datasets for both graph-level and link-level tasks. All the datasets require modeling LRI for accurate prediction on downstream tasks. We aim to provide answers to two following questions. **Q1:** How effective are the proposed methods on real-world molecular datasets with common GNNs? **Q2:** How does the grouping strategy of neural atoms affect the performance of different GNNs for capturing the LRI?

**Setup.** We implement the Neural Atom with GNNs in the GraphGPS framework [14], which provide various choices of positional and structural encodings. All the experiments are run on an NVIDIA RTX 3090 GPU with AMD Ryzen 3960X as the CPU. We employ the molecular datasets (Peptides-Func, Petides-Struct, PCQM-Contact) that exhibit LRI from Long Range Graph Benchmarks (LRGB) [26]. Detailed experiment settings are shown in the appendix B.

**Baseline.** We employ the GCN [11], GINE [9], GCNII [5] and GatedGCN [4] and GatedGCN augmented with Random Walk Structure Encoding (RWSE) as the baseline GNNs. To capture the LRI, one could adopt the fully connected graph to obtain interatomic interaction for distant atom pairs explicitly. Here, we adopt the Graph Transformers for comparison. Specifically, we introduce the fully connected Transforemr [24] with Laplacian Position Encodings [25], SAN [13] and the recent GraphGPS [14], which utilize GNNs and Transformer to capture short-range and long-range information respectively. We cooperate our Neural Atom with different GNN models to evaluate its performance, denoted as + *Neural Atom*.

**Datasets** The statistical information of the datasets is shown as Tab. 1. Note that all three datasets

Table 2: Test performance on three LRGB datasets. Shown is the mean  $\pm$  s.d. of 4 runs.

Model	Peptides-func	Peptides-struct	PCQM-Contact
	AP $\uparrow$	MAE $\downarrow$	MRR $\uparrow$
Transformer+LapPE	0.6326 $\pm$ 0.0126	0.2529 $\pm$ 0.0016	0.3174 $\pm$ 0.0020
SAN+LapPE	0.6384 $\pm$ 0.0121	0.2683 $\pm$ 0.0043	0.3350 $\pm$ 0.0003
GraphGPS	0.6535 $\pm$ 0.0041	0.2500 $\pm$ 0.0005	0.3337 $\pm$ 0.0006
GCN	0.5930 $\pm$ 0.0023	0.3496 $\pm$ 0.0013	0.2329 $\pm$ 0.0009
<b>+ Neural Atoms</b>	<b>0.6220 <math>\pm</math> 0.0046</b>	<b>0.2606 <math>\pm</math> 0.0027</b>	<b>0.2534 <math>\pm</math> 0.0200</b>
GINE	0.5498 $\pm$ 0.0079	0.3547 $\pm$ 0.0045	0.3180 $\pm$ 0.0027
<b>+ Neural Atoms</b>	<b>0.6154 <math>\pm</math> 0.0157</b>	<b>0.2553 <math>\pm</math> 0.0005</b>	<b>0.3126 <math>\pm</math> 0.0021</b>
GCNII	0.5543 $\pm$ 0.0078	0.3471 $\pm$ 0.0010	0.3161 $\pm$ 0.0004
<b>+ Neural Atoms</b>	<b>0.5996 <math>\pm</math> 0.0033</b>	<b>0.2563 <math>\pm</math> 0.0020</b>	<b>0.3049 <math>\pm</math> 0.0006</b>
GatedGCN	0.5864 $\pm$ 0.0077	0.3420 $\pm$ 0.0013	0.3218 $\pm$ 0.0011
<b>+ Neural Atoms</b>	<b>0.6562 <math>\pm</math> 0.0075</b>	<b>0.2585 <math>\pm</math> 0.0017</b>	<b>0.3258 <math>\pm</math> 0.0003</b>
GatedGCN+RWSE	0.6069 $\pm$ 0.0035	0.3357 $\pm$ 0.0006	0.3242 $\pm$ 0.0008
<b>+ Neural Atoms</b>	<b>0.6591 <math>\pm</math> 0.0050</b>	<b>0.2568 <math>\pm</math> 0.0005</b>	<b>0.3262 <math>\pm</math> 0.0010</b>

consist of multiple graphs and are evaluated under the inductive setting, which means that the evaluating portion of the dataset differs from the training counterparts. For the PCQM-Contact dataset, the task is to predict whether the distant node pairs (with more than 5 hops away in a molecular graph) would be in contact with each other in the 3D space, *i.e.*, forming hydrogen bonds, which is the inductive link prediction task. The metric for the performance of the model is measured by the Mean Reciprocal Rank (MRR). Both Peptides-func and Peptides-struct are constructed from the same source but serve different purposes. The Peptides-func is a multi-label graph classification dataset for evaluating the model’s ability to capture molecular properties. We adopt the unweighted mean Average Precision (AP) as the metric. The Peptides-struct is a multi-label graph regression dataset based on the 3D structure of the peptides and uses Mean Absolute Error (MAE) as the metric.

#### 4.1 Quantitative Results

Shown as Tab. 2, all the GNNs achieve significant improvement with the assistance of Neural Atom. The GNNs gain improvement from 8.17% to 12.55% on the peptides-func dataset. The GNNs also receive significant improvement on the peptides-func dataset, at most 27.32% for the GINE model. The improvement for different GNNs on various datasets empirically proves that our proposed Neural Atom can enhance the common GNNs to capture LRI on molecular graphs. Especially for the GatedGCN, which exceeds the Transformer with LapPE on the peptides-func dataset and shows competitive results for the other counterparts on both the peptides-func and PCQM-Contact datasets.

We also notice that more powerful GNNs, especially with edge learning or edge attention filtering mechanisms, could lead to better performance in the scenario with LRI. Compared to other GNN models, the significant improvement of GatedGCN could be the incoming information filtering via the gate mechanism, which allows the neural atoms to obtain representation with rich SRI information.

#### 4.2 The varying choice of $K$

As aforementioned, our method groups the atom in the original molecule into  $K$  Neural Atoms. In considering the varying number of atoms in the molecules, we set hyperparameter  $K$  according to the average number of atoms of the dataset. Here, we demonstrate the effect of different strategies of the  $K$ . The *fixed* strategy is the fixed  $K$ , where we simply set the  $K$  as the proportion to the average number of atoms of the dataset, shown as Fig. 4(a). The *decremental* strategy is that we set the  $k$  as the proportion to the average number of atoms of the dataset at the initial layer, and then each layer is the proportion to the last  $K$ , shown as Fig. 4(b). The *incremental* strategy is the reverse of the *decremental* version, where we set the  $K$  in incremental order, shown as Fig. 4(c). We evaluate different strategies for obtaining the number of Neural Atom on peptides-struct, as shown in Tab. 3.

The *fixed* allows the model to have stable interaction space constructed by the fixed number of Neural Atoms in each layer, most GNNs can benefit from such a setting. Whereas the *decremental*, allows the model to have an inverse pyramid style of the interaction space, and obtain information from local to global. The *incremental* might not be suitable for the LRI scenario, as it might break the local structure by mapping the atom representation to a progressively more complex interaction space.

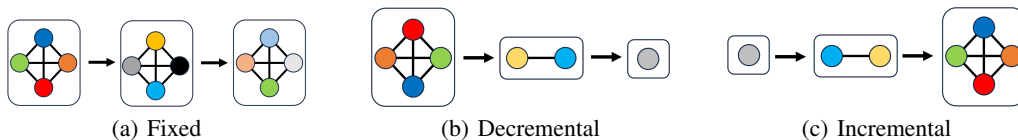


Figure 4: Neural Atom grouping strategies.

Table 3: Test performance for different grouping strategies on **Peptides-struct**.

	Fixed	Incremental	Decremental
GCN	<b>0.2582</b> $\pm$ 0.0011	0.3239 $\pm$ 0.0014	0.2606 $\pm$ 0.0003
GINE	<b>0.2559</b> $\pm$ 0.0001	0.2795 $\pm$ 0.0012	0.2578 $\pm$ 0.0017
GCNII	0.2579 $\pm$ 0.0025	0.4084 $\pm$ 0.0025	<b>0.2563</b> $\pm$ <b>0.0020</b>
GatedGCN	0.2592 $\pm$ 0.0017	<b>0.2568</b> $\pm$ <b>0.0009</b>	<b>0.2569</b> $\pm$ <b>0.0007</b>
GatedGCN+RWSE	<b>0.2521</b> $\pm$ <b>0.0014</b>	0.2600 $\pm$ 0.0012	0.2568 $\pm$ 0.0005

Table 4: Test performance for different values of sparse ratio on **Peptides-func**.

	<i>ratio</i> = 0.1	<i>ratio</i> = 0.5	<i>ratio</i> = 0.9
GCN	0.5859 $\pm$ 0.0073	0.5903 $\pm$ 0.0054	<b>0.6220</b> $\pm$ <b>0.0046</b>
GINE	0.6128 $\pm$ 0.0060	0.6147 $\pm$ 0.0121	<b>0.6154</b> $\pm$ <b>0.0157</b>
GCNII	0.5862 $\pm$ 0.0066	0.5909 $\pm$ 0.0099	<b>0.5996</b> $\pm$ <b>0.0033</b>
GatedGCN	0.6533 $\pm$ 0.0030	<b>0.6562</b> $\pm$ <b>0.0044</b>	<b>0.6562</b> $\pm$ <b>0.0075</b>
GatedGCN+RWSE	0.6550 $\pm$ 0.0032	0.6565 $\pm$ 0.0074	<b>0.6591</b> $\pm$ <b>0.0050</b>

Table 5: Running time comparison and relative improvements for GNNs with *Neural Atom* and Graph Transformers. Average epoch time (average of 5 epochs, including validation performance evaluation) is shown for each model and dataset combination. The GTs are compared to the average time and performance of the three shown GNNs. Full results can be found in the Appendix. B.1.

	GINE	GCNII	GatedGCN	Transformer+LapPE	SAN+LapPE
Peptides-func	(+2.2s, 11.90% $\uparrow$ )	(+2.2s, 11.90% $\uparrow$ )	(+2.8s, 11.90% $\uparrow$ )	(+3.6s, 12.26% $\uparrow$ )	(+57.2s, 13.29% $\uparrow$ )
Peptides-struct	(+1.6s, 27.32% $\downarrow$ )	(+2.8s, 26.16% $\downarrow$ )	(+2.3s, 24.88% $\downarrow$ )	(+3.5s, 27.30% $\downarrow$ )	(+54.8s, 22.88% $\downarrow$ )

We conducted an experiment on the impact of varying proportions, shown in Tab. 4. Smaller grouping ratios lead to more aggressive grouping strategies and vice versa for more moderate ones. We notice that more moderate grouping gives better results. Since the grouping operation potentially coarsens the molecular graph, which could lead to better preservation of the local structure, *i.e.*, the SRI.

To demonstrate the efficiency of our proposed neural atom, we calculate the running time for each training epoch, shown in Tab. 5. Despite the minor additional time-consuming, our method is more computationally efficient than the Transformer approach, especially for the SAN with LapPE.

## 5 Understanding

To illustrate the effect of our neural atom for grouping atoms and providing high-level connections between them, as well as the ability to group meaningful atom groups, we adopt the Mutagenicity dataset [19] as it provides interpretable atom group labels for the molecular graph category, where  $-NO$  and  $-NH_2$  are accounted for the *mutagen* property of the given molecule.

To visualize the potential interatomic interactions, we adopt the Ewald sum matrix as the indicator. Each element in the Ewald sum matrix is an Ewald Summation for the specific interatomic interaction, indicated by the row and column index of the Ewald sum matrix. Here, we leverage a three-layer GIN [31] model with a fixed amount of neural atoms (four neural atoms in our case) for each layer. We visualize the neural atom allocation matrix by assigning a unique color to each atom in the original molecular graph, according to the index of the largest attention weight of the matrix.

Shown as Fig. 5(a) to 5(c), we visualize the allocation pattern for the neural atoms at each layer along with the interatomic interactions indicated by the Ewald sum matrix. At the initial layer, all hydrogen atoms (H) are grouped into the same neural atom, which allows the model to obtain information about H at different locations on the graph. The nitrogen atoms (N) are categorized as an individual

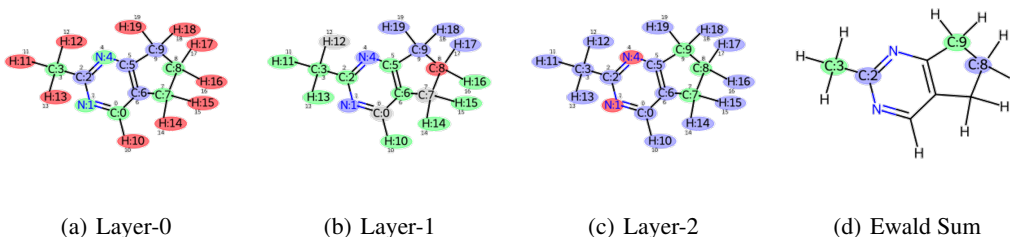


Figure 5: Neural Atom grouping pattern at each layer for non-mutagen molecular

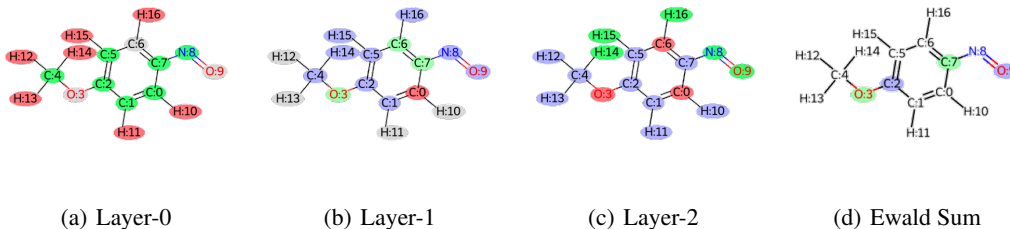


Figure 6: Neural Atom grouping pattern at each layer for mutagen molecular ( $-NO$ )

neural atom, which allows different nodes on the graph to interact with it directly via the neural atom they belong to. In the last layer, most atoms are categorized into the same neural atom, providing a global representation of the graph, while N is still categorized as a separate class so that its unique information can be preserved. The grouping pattern also aligns with the interatomic interaction indicated by the Ewald sum matrix, where we apply thresholding for visual simplicity. Atoms with the same color in Fig. 5(d) indicate that they exhibit strong interaction potential. Shown as Fig. 5, the corresponding atom within (C:3-C:9) and (C:2-C:8) are grouped into two different neural atoms, allowing the model to capture their interaction via the information exchanging between neural atoms.

In addition, we visualize the mutagen molecular with  $-NO$ , shown as Fig. 6. At the initial layer, hydrogen atoms (H) and oxygen atoms (O) are all grouped into individual Neural Atoms despite the multi-hop distance between them. This allows the model to capture the atom representation for each element. In the rest of the layers, the elements of  $-NO$  (N:8 and O:9) are grouped into Neural Atom, allowing the model to capture their representation as a whole, which serves for the prediction of the molecular graph. Note that the grouping pattern is also aligned with the interatomic interaction indicated by the Ewald sum matrix. The corresponding atoms within (C:2-O:9) and (C:7-O:3) are grouped into two different Neural Atom, the model can capture the LRI despite the hops distance and the intermediate atoms between them. The visualization demonstrates our method can bridge the distant atom and the atom groups could contribute to the prediction of the molecular graph properties.

## 6 Discussion and Conclusion

**Limitation.** This work mainly focuses on the molecular graph without 3D coordinate information, which could benefit the incorporation of LRI, as it depends on the interatomic distance in 3D space. In addition, our work pays close attention to the intra-molecular interaction rather than the inter-molecular interaction, where more valuable information might lie. For example, protein docking also involves the formation of the hydrogen bond between two biochemical components [29].

**Extension.** One intuitive approach is extending the *Neural Atom* to leverage the atomic coordinate information better to capture the LRI. The *Neural Atom* can also model the inter-molecular interaction by extending to the 3D scenario. Another possible direction is to instill expert knowledge in the grouping strategy to improve the interpretation ability and discriminability of the grouped atoms.

**Conclusion.** In this study, we aim to enhance GNNs to capture long-range interactions better. We achieve this by transforming original atoms into neural atoms, facilitating information exchange, and then projecting the improved information back to atomic representations. This novel approach reduces interaction distances between nodes to a single hop. Extensive experiments on three long-range graph benchmarks validate our method’s ability to enhance any GNN to capture long-range interactions.

## References

- [1] U. Alon and E. Yahav. On the bottleneck of graph neural networks and its practical implications. In *ICLR*, 2020.
- [2] J. Ba, J. Kiros, and G. Hinton. Layer normalization. [arXiv:1607.06450](https://arxiv.org/abs/1607.06450), 2016.
- [3] J. Baek, M. Kang, and S. Hwang. Accurate learning of graph representations with graph multiset pooling. In *ICLR*, 2021.
- [4] X. Bresson and T. Laurent. Residual gated graph convnets. [arXiv:1711.07553](https://arxiv.org/abs/1711.07553), 2017.
- [5] M. Chen, Z. Wei, Z. Huang, B. Ding, and Y. Li. Simple and deep graph convolutional networks. In *ICML*, 2020.
- [6] R. Ekagra, S. Soumya, and T. Partha. ASAP: Adaptive structure aware pooling for learning hierarchical graph representations. In *AAAI*, 2020.
- [7] F. Faber, A. Lindmaa, O. A. Von L., and R. Armiento. Crystal structure representations for machine learning models of formation energies. *IJQC*, 115(16):1094–1101, 2015.
- [8] M. Gromiha and S. Selvaraj. Importance of long-range interactions in protein folding. *Biophysical chemistry*, 77(1):49–68, 1999.
- [9] W. Hu, B. Liu, J. Gomes, M. Zitnik, P. Liang, V. Pande, and J. Leskovec. Strategies for pre-training graph neural networks. In *ICLR*, 2020.
- [10] V. Ioannidis, D. Zheng, and G. Karypis. Few-shot link prediction via graph neural networks for covid-19 drug-repurposing. [arXiv:2007.10261](https://arxiv.org/abs/2007.10261), 2020.
- [11] T. Kipf and M. Welling. Semi-supervised classification with graph convolutional networks. In *ICLR*, 2016.
- [12] A. Kosmala, J. Gasteiger, N. Gao, and S. Günnemann. Ewald-based long-range message passing for molecular graphs. [arXiv:2303.04791](https://arxiv.org/abs/2303.04791), 2023.
- [13] D. Kreuzer, D. Beaini, W. Hamilton, V. Létourneau, and P. Tossou. Rethinking graph transformers with spectral attention. In *NeurIPS*, 2021.
- [14] R. Ladislav, M. Galkin, D. Prakash, L. Tuan, W. Guy, and B. Dominique. Recipe for a general, powerful, scalable graph transformer. In *NeurIPS*, 2022.
- [15] D. Leeson and J. Young. Molecular property design: does everyone get it?, 2015.
- [16] Z. Li, M. Jiang, S. Wang, and S. Zhang. Deep learning methods for molecular representation and property prediction. *Drug Discovery Today*, page 103373, 2022.
- [17] S. Liu, H. Wang, W. Liu, J. Lasenby, H. Guo, and J. Tang. Pre-training molecular graph representation with 3d geometry. In *ICLR*, 2022.
- [18] Y. Ma, S. Wang, C. Aggarwal, and J. Tang. Graph convolutional networks with eigenpooling. In *KDD*, 2019.
- [19] C. Morris, N. Kriege, F. Bause, K. Kersting, P. Mutzel, and M. Neumann. Tudataset: A collection of benchmark datasets for learning with graphs. In *ICML Workshop on Graph Representation Learning and Beyond*, 2020.
- [20] M. Rycker, B. Baragaña, L. Duce, and I. Gilbert. Challenges and recent progress in drug discovery for tropical diseases. *Nature*, 559(7715):498–506, 2018.
- [21] H. Stärk, D. Beaini, G. Corso, P. Tossou, C. Dallago, S. Günnemann, and P. Liò. 3d infomax improves gnn for molecular property prediction. [arXiv:2110.04126](https://arxiv.org/abs/2110.04126), 2021.
- [22] J. Thomas, A. Moallem-Oureh, S. Beddar-Wiesing, and C. Holzhüter. Graph neural networks designed for different graph types: A survey. *Transactions on Machine Learning Research*, 2023.

- [23] A. Toukmaji and J. Board Jr. Ewald summation techniques in perspective: a survey. Computer physics communications, 95(2-3):73–92, 1996.
- [24] A. Vaswani, N. Shazeer, N. Parmar, J. Uszkoreit, L. Jones, N. Gomez, Ł. Kaiser, and I. Polosukhin. Attention is all you need. In NeurIPS, 2017.
- [25] D. Vijay, L. Anh, L. Thomas, B. Yoshua, and B. Xavier. Graph neural networks with learnable structural and positional representations. In ICLR, 2022.
- [26] D. Vijay, R. Ladislav, G. Mikhail, P. Ali, W. Guy, L. Anh, and B. Dominique. Long range graph benchmark. In NeurIPS Datasets and Benchmarks Track, 2022.
- [27] O. Wieder, S. Kohlbacher, M. Kuenemann, A. Garon, P. Ducrot, T. Seidel, and T. Langer. A compact review of molecular property prediction with graph neural networks. Drug Discovery Today: Technologies, 37:1–12, 2020.
- [28] W. Winterbach, P. Mieghem, M. Reinders, H. Wang, and D. Ridder. Topology of molecular interaction networks. BMC systems biology, 7:1–15, 2013.
- [29] M. Wu, D. Dai, and H. Yan. Prl-dock: Protein-ligand docking based on hydrogen bond matching and probabilistic relaxation labeling. Proteins: Structure, Function, and Bioinformatics, 80(9):2137–2153, 2012.
- [30] Z. Wu, S. Pan, F. Chen, G. Long, C. Zhang, and P. Yu. A comprehensive survey on graph neural networks. IEEE transactions on neural networks and learning systems, 32(1):4–24, 2020.
- [31] K. Xu, W. Hu, J. Leskovec, and S. Jegelka. How powerful are graph neural networks? In ICLR, 2018.
- [32] C. Ying, T. Cai, S. Luo, S. Zheng, G. Ke, D. He, Y. Shen, and T. Liu. Do transformers really perform badly for graph representation? In NeurIPS, 2021.
- [33] Z. Ying, J. You, C. Morris, X. Ren, W. Hamilton, and J. Leskovec. Hierarchical graph representation learning with differentiable pooling. In NeurIPS, 2018.
- [34] Y. Zhang, Y. Hu, N. Han, A. Yang, X. Liu, and H. Cai. A survey of drug-target interaction and affinity prediction methods via graph neural networks. Computers in Biology and Medicine, page 107136, 2023.
- [35] Z. Zhang, L. Chen, F. Zhong, D. Wang, J. Jiang, S. Zhang, H. Jiang, M. Zheng, and X. Li. Graph neural network approaches for drug-target interactions. Current Opinion in Structural Biology, 73:102327, 2022.

# Appendix

## A Long Range Interaction examples

The long-range interaction affects the surface area of the molecule or contributes to the formation of hydrogen bonds, which in turn affects the properties, such as melting point, water affinity, viscosity, of the molecule [32; 17; 21; 8]. Understanding and quantifying these long-range interactions is crucial in chemistry, physics, and materials science, as they influence the behavior and properties of molecules, materials, and biological systems. Here, we show different types of LRI and their properties.

- **Van der Waals Force** is a weak attractive interaction that occurs between all atoms and molecules. These forces arise due to temporary fluctuations in electron distribution, creating temporary dipoles. Van der Waals forces include London dispersion forces (arising from instantaneous dipoles), dipole-dipole interactions, and induced dipole-induced dipole interactions. These forces can act over relatively long distances and are responsible for the condensation of gases into liquids.
- **Hydrogen Bond** is a special type of dipole-dipole interaction that occurs when hydrogen is bonded to a highly electronegative atom (such as oxygen, nitrogen, or fluorine) and is attracted to another electronegative atom in a nearby molecule. Hydrogen bonds are relatively strong compared to other long-range interactions and play a crucial role in the structure and properties of water, DNA, and proteins.

**Electrostatic Interaction**, also known as Coulombic interactions, occur between charged particles. While ionic bonds are a type of strong electrostatic interaction, long-range electrostatic interactions can also occur between charged ions or polar molecules that are not directly bonded to each other. These interactions can be both attractive and repulsive, depending on the charges involved.

**Dipole-Dipole Interaction** occurs between molecules that have permanent dipoles, meaning they have a separation of positive and negative charges within the molecule. These interactions are stronger than van der Waals forces and can act over longer distances.

**Ion-Dipole Interaction** occurs when an ion interacts with the dipole moment of a polar molecule. These interactions are important in solutions where ions are dissolved in a polar solvent.

**Dispersion Interaction**, also known as London dispersion forces, is a component of van der Waals forces. They arise from temporary fluctuations in electron distribution and can act between all molecules, even non-polar ones. These forces can be relatively weak but can accumulate to have a significant impact on molecular interactions.

**Magnetic Interaction** is a long-range magnetic interaction that can occur between magnetic moments associated with atoms or ions. These interactions are responsible for the behavior of ferromagnetic and antiferromagnetic materials.

## B Reproduction details

We performed our experiment on four seeds and reported the mean with standard deviation as the final result. We summarize the common hyperparameters that are shared across different models on the introduced datasets, along with the model-specific hyperparameters, shown as Tab. 6 to Tab. 9.

### B.1 Running time for different models

We show the running time for different models in Tab. 10, training with the hyperparameters given as Tab. 6 to Tab. 9.

Table 6: Common hyperparameters for datasets from Long Range Graph Benchmark.

Hyperparameter	PCQM-Contact	Peptides-func	Peptides-struct
Dropout	0	0.12	0.2
Allocation matrix Grouping	mean	mean	mean
Positional Encoding	LapPE-10	LapPE-10	LapPE-10
PE dim	16	16	20
PE encoder	DeepSet	DeepSet	DeepSet
Batch size	256	128	128
Learning Rate	0.001	0.0003	0.0003
# Epochs	200	200	200

Table 7: Model-specific hyperparameters for PCQM-Contact

Hyperparameter	# GNN Layers	Hidden dim	# Heads	ratio
GCN	5	300	1	0.9
GCNII	5	100	2	0.8
GINE	5	100	1	0.95
GatedGCN	8	72	1	0.5

Table 8: Model-specific hyperparameters for Peptides-func

Hyperparameter	# GNN Layers	Hidden dim	# Heads	ratio
GCN	5	155	1	0.15
GCNII	5	88	1	0.2
GINE	5	88	2	0.9
GatedGCN	5	88	1	0.5

Table 9: Model-specific hyperparameters for Peptides-struct

Hyperparameter	# GNN Layers	Hidden dim	ratio
GCN	5	155	1 0.15
GCNII	5	88	1 0.2
GINE	5	88	2 0.9
GatedGCN	5	88	1 0.5

Table 10: Wall-clock run times. Average epoch time (average of 5 epochs, including validation performance evaluation) is shown for each model and dataset combination.

avg. time / epoch	Peptides-func	Peptides-struct	PCQM-Contact
GCN	2.6s	2.5s	56.9s
+ Neural Atom	5.5s	4.9s	65.1s
GINE	2.6s	2.6s	56.7s
+ Neural Atom	4.8s	4.2s	66.8s
GCNII	2.5s	2.3s	56.9s
+ Neural Atom	4.7s	5.1s	59.4s
GatedGCN	3.3s	3.2s	56.5s
+ Neural Atom	6.1s	5.5s	61.6s
GatedGCN+RWSE	3.4s	4.1s	59.4s
+ Neural Atom	6.4s	5.2s	65.0s
Transformer+LapPE	6.4s	6.2s	59.2s
SAN+LapPE	60s	57.5s	205s
GraphGPS	6.5s	6.5s	61.5s